VIGR – a novel inducible adhesion family G-protein coupled receptor in endothelial cells ☆,☆☆

Christian Stehlik[1], Renate Kroismayr, Andrea Dorfleutner, Bernd R. Binder, Joachim Lipp*

Department of Vascular Biology and Thrombosis Research, Medical University of Vienna, and BMT – Biomolecular Therapeutics GmbH, Brunnerstrasse 59, A-1235 Vienna, Austria

Received 30 January 2004; revised 14 May 2004; accepted 18 May 2004

Available online 5 June 2004

Edited by Beat Imhof

Abstract Using a signal sequence trap for selection of differentially expressed secretory and membrane proteins, we identified a novel member of the adhesion family of G-protein coupled receptors (GPCRs), termed vascular inducible GPCR (VIGR). VIGR contains C1r-C1s, Uegf and Bmp1 (CUB) and pentraxin (PTX)-like modules and a mucin-like spacer, followed by seven transmembrane domains. By surface biotinylation as well as by immunofluorescence analysis we demonstrate that endogenous, highly glycosylated VIGR is expressed on the cell surface of endothelial cells (ECs) upon LPS or thrombin treatment, and inducible expression is mediated by MAP kinases, but not NF-κB. We show that VIGR is selectively expressed in ECs derived from larger vessels, but not from microvessels. In summary, VIGR represents a novel GPCR of the adhesion family, which is unique in its long extra-cellular domain comprising CUB and PTX-like modules and in its inducibility by LPS and thrombin in a subset of ECs, suggesting an important function in cell-adhesion and potentially links inflammation and coagulation.

Keywords: Inflammation; Adhesion; G-protein coupled receptor; C1r-C1s, Uegf and Bmp1; Pentraxin; Endothelial cell; Mitogen-activated protein kinase

1. Introduction

The vascular endothelium is located at the interface between the bloodstream and the body tissues and plays an active and central role in the process of acute inflammation by controlling the transmigration of leukocytes through the EC layer and the flux into an inflammatory nidus [1]. Many of the proteins involved are either up- or down-regulated in response to pro-inflammatory stimuli, including cytokines, secreted proteases and receptors.

G-protein coupled receptors (GPCRs) represent the most diverse protein family in structure as well as in function [2] and couple to second messenger cascade mechanisms, such as cyclic AMP, inositol phosphate, calcium ions, or diacylglycerol, through heterotrimeric G proteins, though, signals may be also transmitted via other, non G-protein effector molecules [2,3]. GPCRs can process a wide variety of exogenous stimuli including hormones, cytokines, peptides, amino acid derivates, ions, neurotransmitters and sense dependent stimuli to mediate signal transduction. Altogether five families of GPCRs can be distinguished, including glutamate, rhodopsin, adhesion, frizzled/taste2, and secretin, accordingly to the GRAFS classification system [4].

The steadily growing family of adhesion GPCRs (formerly known as secretin-like, B2, EGF-TM7, LNB-7TM, or LN-7TM), are intriguing receptors with evidence of participation in lymphocyte activation, macrophage biology, synaptic exocytosis and planar polarization during organogenesis [5–7]. Recent evidence suggests that at least 30 family members are encoded in the human genome [8]. These receptors are characterized, besides their heptahelical domain, by the presence of a long extracellular domain built of adhesion motifs, such as EGF, cadherin, lectin, laminin, olfactomedin, immunoglobulin, integrin-binding, or thrombospondin domains, a highly glycosylated, proline-rich mucin-like region that is linked to the heptahelical domain via the GPCR proteolytic site (GPS) [5–7]. Proteolytic cleavage of the GPS might result in shedding of the receptor from the plasma membrane giving raise to a soluble α-subunit, which is non-covalently linked to the β-subunit comprised of the heptahelical domain and the cytoplasmic tail [9–14]. Also the conserved cysteine residues localized in the first and second extracellular loop that apparently form a disulfide bond to stabilize the tertiary structure, are found in the adhesion class of GPCRs. Receptors of this family, such as CD97 and EMR2-4 have indeed been shown to bind to other cell surface proteins and extracellular matrix proteins via their adhesion modules in the extracellular domain [11,15–20]. To

☆ Supplementary data associated with this article can be found, in the online version, at doi:10.1016/j.febslet.2004.05.038.
☆☆ GenBank Accession No.: AF216967.

* Corresponding author. Fax: +43-1-4277-62550.
E-mail addresses: cstehlik@hsc.wvu.edu (C. Stehlik), adorfleutner@hsc.wvu.edu (A. Dorfleutner), hans-joachim.lipp@meduniwien.ac.at (J. Lipp).

[1] Present address: Mary Babb Randolph Cancer Center and Department of Microbiology, Immunology, and Cell Biology, West Virginia University School of Medicine, P.O. Box 9300, Morgantown, WV 26506, USA. Fax: +1-304-293-8785 (C. Stehlik), Fax: +1-304-293-0501 (A. Dorfleutner).

Abbreviations: CUB, C1r-C1s, Uegf and Bmp1; HAECs, human aortic ECs; HUVECs, human umbilical vein ECs; HSMECs, human skin microvascular ECs; EC, endothelial cell; GPCR, G-protein coupled receptor; GPS, GPCR proteolytic site; LPS, lipopolysaccharide; MAPKs, mitogen-activated protein kinases; NF-κB, nuclear factor kappaB; PTX, pentraxin-like domain; TNF, tumor necrosis factor; VIGR, vascular inducible GPCR

0014-5793/$22.00
doi:10.1016/j.febslet.2004.05.038

understand the complex responses of ECs to pro-inflammatory stimuli and the mechanisms underlying the resulting intercellular cross talk, we were interested in differentially expressed secretory and membrane proteins in activated ECs, which we selected using a novel signal sequence trap.

2. Materials and methods

2.1. Vector construction and functional screen for signal sequences and transmembrane domains

Plasmids pAP1, pAP2, and pAP3 were constructed using pTrc99A (Roche) and pMG [21]. These plasmids contain a signal sequence deleted form of the bacterial alkaline phosphatase A encoding gene AP [21] and a multiple cloning site in all three reading frames. cDNA libraries derived from human umbilical vein ECs (HUVECs) were amplified by PCR and cloned in all three reading frames into pAP1-3. *Escherichia coli* DH5α were transformed by electroporation using Gene Pulser (Bio-Rad) at 25 μF/200 Ω/1.5 kV and 0.1 cm electrode gap cuvettes (Bio-Rad) and were selected with 50 μg/ml ampicillin, 100 mM isopropyl-β-D-thiogalactopyranoside, and 40 μg/ml 5-bromo-4-chloro-3-indolyl-phosphate (XGAL). Bacterial colonies, which express an AP gene with a functionally restored signal sequence, were detected when growing in presence of the chromogenic AP-substrate XGAL. Positive clones were analyzed by DNA sequencing.

2.2. Northern-, Southern-, and dot-blot hybridization

Hybridizations were carried out using QuickHyb solution (Stratagene) under high stringent conditions according to the manufacturers instructions and signals were analyzed on a PhosphoImager SF (Molecular Dynamics). Total RNA and genomic DNA were isolated using Trizol reagent (Gibco-BRL) and mRNA was isolated using Dynabeads (Dynal). cDNA probes and mRNAs were labeled by random priming (Stratagene) and reverse transcription (Roche) in the presence of [α-^{32}P]dATP, respectively.

2.3. Cell culture and metabolic labeling of cells

Human ECs were grown in gelatin-coated flasks in M199-medium/20% SCS (HyClone)/endothelial cell growth factor supplement (ECGF) (Technoclone, Vienna, Austria)/Penicillin/Streptomycin/Fungizone (Bio Whittaker)/3 U/ml heparin (Roche). Where indicated cells have been treated with LPS (lipopolysaccharide, 600 ng/ml), TNFα (tumor necrosis factor α, 500 U/ml), CHX (cycloheximide, 10 μg/ml), IL-1β (Interleukin-1β, 300 U/ml), IL-6 (200 U/ml), IL-8 (200 ng/ml), IL-10 (2 ng/ml), EGF (epidermal growth factor, 10 ng/ml), TGFβ (transforming growth factor β, 2 ng/ml), thrombin (4 U/ml), VEGF (vascular endothelial growth factor, 1.25 nM), OM (oncostatin M, 20 ng/ml), PMA (phorbol 12-myristate 13-acetate, 20 ng/ml), or IF-α (interferon-α, 1000 U/ml). HUVECs were metabolically labeled with 50 μCi/ml Pro-mix L-[^{35}S] (Amersham–Pharmacia Biotech) in Cys/Met-deficient RPMI 1640 medium (Gibco-BRL) supplemented with 5% SCS (HyClone)/ECGF (Technoclone, Vienna, Austria)/Penicillin/Streptomycin/Fungizone (Bio Whittaker)/heparin (3 U/ml, Roche) for 16 h. All batches of ECs were tested routinely for their inducibility in response to pro-inflammatory stimuli, employing an ELAM-1 ELISA test.

2.4. cDNA cloning and sequencing

HUVEC and placenta lambda cDNA libraries (Clontech) were screened with a 300 bp [α-^{32}P]dATP labeled cDNA probe (prime-it II, Stratagene) specific to the heptahelical domain of vascular inducible GPCR (VIGR) using QuickHyb solution (Stratagene) at 65 °C according to the manufacturer's instructions, and a 1.3 kb cDNA was identified. This cDNA fragment was elongated by 3′ and 5′ RACE methods. A list of primers is given in the on-line supplement. Obtained PCR fragments were cloned into pGEM vectors (Promega) and sequenced using the ABI PRISM system and a 373A DNA sequencer (both Perkin–Elmer).

2.5. Generation and affinity-purification of polyclonal antibodies

A recombinant VIGR protein, comprised of a part of the extracellular domain (7TM: aa 625-745) in pQE31 (Qiagen), was expressed and purified from *E. coli* M15 (Qiagen) as a 6× His-tagged fusion protein. Branched peptides (P3: WGPPDISNCSREA, aa 544–556; P4: GLPSNNESY, aa 671–679; C1: VKGYCNAHSDNFYK, aa 1195–1208; C2: GRFRLADNSDWSKT, aa 1104–1117) were synthesized (Research Genetics) and either 225 μg of these branched, unconjugated peptides without a carrier protein or 100 μg of the 6× His-fusion protein were directly used for immunization of rabbits with Complete Freund's adjuvant and three times booster immunizations in 4 week intervals using Incomplete Freund's adjuvant. The resulting antisera were affinity-purified using either the immobilized peptides or the fusion protein. For immunoprecipitation experiments, 2–3 μg of purified antibodies (C2 or 7TM) were used. In immunofluorescence studies, the P4 antibody was applied at a concentration of 5 μg/ml.

2.6. Biotinylation of cell surface proteins and immunoprecipitation

To biotinylate cell surface proteins, cells were washed with ice-cold PBS and incubated with 0.5 mg/ml of Sulfo-NHS-LC-Biotin (Pierce) in PBS for 40 min at 4 °C. Cells were washed and lysed using 1% sucrose monolaurate buffer (150 mM NaCl/5 mM $MgCl_2$/50 mM Tris/HCl, pH 7.5/20 μg/ml PMSF) and cleared by centrifugation. 300 μg or 10^7 cpm of protein lysate were pre-cleared with Protein A–Sepharose at 4 °C for 30 min and immunoprecipitated at 4 °C o/n. Immune complexes were washed three times with 0.2% NP-40/10 mM Tris, pH 7.5/150 mM NaCl/2 mM EDTA, twice with 0.2% NP-40/10 mM Tris, pH 7.5/500 mM NaCl/2 mM EDTA, once with 10 mM Tris pH 7.5 and analyzed by SDS–PAGE followed by either autoradiography or immunoblotting using streptavidin–peroxidase conjugate (Roche) and ECL plus (Amersham–Pharmacia Biotech).

2.7. Treatment of HUVECs with chemical inhibitors

HUVECs were treated with LPS alone or in combination with either 5 μM of the specific nuclear factor kappaB (NF-κB) inhibitor BAY11-7082 (Alexis), 50 μM of the specific MEK1 inhibitor PD98059 (Tocris), 40 μM of the specific p38 MAPK inhibitor SB202190 (Tocris), or 25 μM of the specific JNK inhibitor SP600125 (Tocris) for 16 h. Inhibitors were added to the culture medium 1 h prior to LPS stimulation. Biotinylation and immunoprecipitation was carried out as described above.

2.8. Deglycosylation by tunicamycin treatment

Where indicated, HUVECs were treated with LPS and 4 μg/ml tunicamycin (Roche) for 16 h.

2.9. Immunofluorescence

HUVECs were grown on fibronectin (Sigma) coated Permanox chamber slides (Lab-Tek), treated with LPS for 16 h or left untreated, then washed with PBS supplemented with 0.5% FBS and 0.1% BSA and stained with an indirect labeling method by incubating first with the affinity purified anti-VIGR-P4 antibody in 0.1% BSA in PBS at 4 °C for 2 h, washed and stained with a FITC-anti-rabbit secondary antibody (Molecular Probes). Stained cells were then fixed with 70% ethanol at 4 °C o/n. Following washing three times with ice-cold PBS, slides were mounted and visualized under a fluorescence microscope.

2.10. ELAM-1 ELISA

HUVECs were seeded into 96-well plates and confluent cell layers were stimulated with LPS for 4 h. Cells were fixed using 0.1% glutaraldehyde for 15 min at 4 °C and subsequently incubated in 5% BSA for 1 h. ELAM-1 expression is detected by using anti-ELAM-1 antibody (R&D Systems) and a goat anti-mouse-HRP conjugate (Amersham–Pharmacia). After incubation with OPD substrate (Sigma), the reaction was stopped by addition of H_2SO_4 and absorption by 492 nm was measured. All samples were done in duplicates.

3. Results

3.1. Molecular cloning of VIGR, a novel member of the adhesion class of the GPCR super-family

We employed a two-step signal sequence trap procedure to identify differentially expressed secretory and transmembrane proteins in endothelial cells (ECs) (C. Stehlik, B.R. Binder, and J. Lipp, manuscript submitted). First, cDNAs were screened

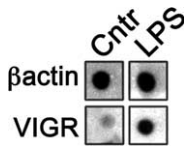

Fig. 1. Dot-blot analysis of *VIGR* cDNA. Bacterial colonies were grown on nylon membranes and hybridized to reverse transcribed, [α-^{32}P]dATP labeled mRNA isolated from either resting or 12 h LPS-treated HUVECs. Colonies containing β-*actin* cDNA-fragments were used as control.

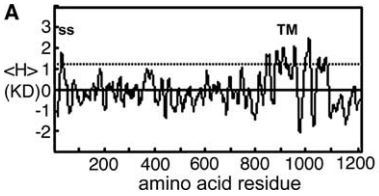

B

	h	m	
h		74.8 79.9	% identity % similarity
r	69.3 73.9	77.9 80.1	% identity % similarity

Fig. 2. (A) The hydropathy profile of human VIGR according to Kyte and Doolittle. Signal sequence (ss), transmembrane domain (TM). (B) Percentage of amino acid identity and similarity for human, mouse and rat VIGR proteins.

for the presence of sequences that are able to provide signal sequence function, employing pAP plasmids as a vector. Bacterial alkaline phosphatase A (AP) lacking its signal sequence was used as a reporter gene to identify cDNA fragments that can restore signal sequence function, employing a chromogenic AP-substrate. In a second step we screened the candidate genes whether they are differentially expressed in response to pro-inflammatory stimuli in ECs by dot-blot analysis (Fig. 1). Selected bacteria were grown on grid-containing agar plates, transferred to nylon membranes and hybridized with ^{32}P-labelled cDNA derived from resting or LPS-stimulated HUVECs.

One of the identified proteins was VIGR, showing similarity to the adhesion GPCRs, which are believed to be involved in cell adhesion [5–7]. The full-length cDNA of 4.7 kb encodes an open reading frame of 1222 amino acids and a deduced protein of ~136 kDa. A hydropathy profile of VIGR predicted a hydrophobic signal sequence at the N-terminus and seven transmembrane-spanning domains at the C-terminus (Fig. 2A). The highest overall identity of 39% and 31% was found to HE6 and CD97, respectively [22,23]. Amino acid sequence analysis revealed all the characteristics of the adhesion class of GPCRs, including a signal peptide, a long, highly glycosylated extracellular domain with 27 putative N-glycosylation sites, and a GPS. Within the heptahelical domain two conserved cysteine residues are present, which are thought to form a disulfide bridge between the first and second extracellular loop that have been shown to be critical for the function of the secretin receptor [24]. When compared to other family members of the adhesion class of GPCRs, two not yet documented protein motifs are found in the extracellular portion, namely a C1r-C1s, Uegf and Bmp1 (CUB) (aa residues 41–149) and a pentraxin (PTX)-like (aa residues 150–355) domain. Two cysteine residues forming a potential palmitoylation site are found in the long cytoplasmic domain which also contains several potential phosphorylation sites for cAMP dependent kinases/protein kinase G, protein kinase C, casein kinase II, as well as a potential myristoylation signal and a microbodies C-terminal targeting motif.

Predicted *VIGR* orthologues are encoded in the mouse (XM136924) and rat (XM218313) genome, sharing between 69% and 78% identity, and between 73% and 80% similarity, respectively (Fig. 2B).

3.2. Chromosomal localization, genomic organization and tissue distribution of VIGR

Southern-blot analysis of human genomic DNA revealed a single copy gene that we mapped to chromosome 6 by Southern-blot analysis of a *Pst*I digested Somatic Cell Hybrid Panel (Oncor) (Fig. 3A and data not shown). A 135 kb (AL033377) genomic sequence of chromosome 6q23.1–24.3 revealed that the *VIGR* gene is organized in 24 exons spanning 133.9 kbp of genomic DNA (Fig. 3B). By sequence analysis and comparison to the human genome, the genomic structure of VIGR was verified and the intron/exon boundaries were determined (Fig. 3C). All introns are flanked by the splicing consensus sequences, GT at the start and AG at the end of the intron. Similarly, mouse and rat *vigr* are encoded in 23 exons spanning 69,4 kbp on band A2 on the syntenic mouse chromosome 10, and 64 kbp on the syntenic rat chromosome 1p13, respectively. However, in mouse and rat, the signal peptide is encoded in just two exons, thus missing exon 2. Northern-blot analysis revealed three *VIGR* transcripts of approximately 4.7, 7.7, and 9 kb in placenta and to a lower extent in pancreas and liver (Fig. 3D). These transcripts most likely represent alternatively spliced iso-forms or utilization of alternative polyadenylation signals.

3.3. Expression of VIGR is EC-type specific and inducible

We identified *VIGR* as a differentially expressed gene in activated primary human ECs, therefore we tested the expression in response to a variety of inflammatory stimuli. In HUVECs, *VIGR* responded to LPS and thrombin, but not to other inflammatory stimuli, with clearly elevated mRNA levels detectable after 4 h, peaking at 12 h, and declining to background levels at 24 h of LPS treatment (Fig. 4A). When we performed similar time course experiments using primary ECs of different origin we could not detect any transcripts in skin microvascular ECs (Fig. 4B, right panel). However, constitutive expression of the 4.7 kb transcript was detectable in aortic ECs (Fig. 4C). The discrepancy between inducibility of *VIGR* expression in skin-microvascular derived ECs to umbilical vein derived ECs was also observed in EC lines generated by infection with an amphotrophic helper free recombinant retrovirus construct, pLXSN16 E6/E7, containing the E6/E7 open reading frame of human papilloma virus 16 (personal gift, Renate Hofer-Warbinek). None of the skin microvascular EC derived lines, named HM2, HM39/2, and HM60, were found to express *VIGR* in response to LPS stimulation (data not shown), whereas the HUVEC derived line HU2 was able to express *VIGR* upon LPS stimulation (data not shown). Results obtained by Northern-blot analysis were similar to the results shown in Fig. 4 for the primary cells. All these cell lines were tested positively for expression of adhesion molecules upon pro-inflammatory stimuli, the ability of tube formation and LDL uptake and reflect typical endothelial cell behaviour regarding these aspects.

3.4. VIGR is a highly glycosylated cell surface protein

To analyze VIGR protein, we raised polyclonal rabbit antibodies either directed to the extracellular- (P3,P4),

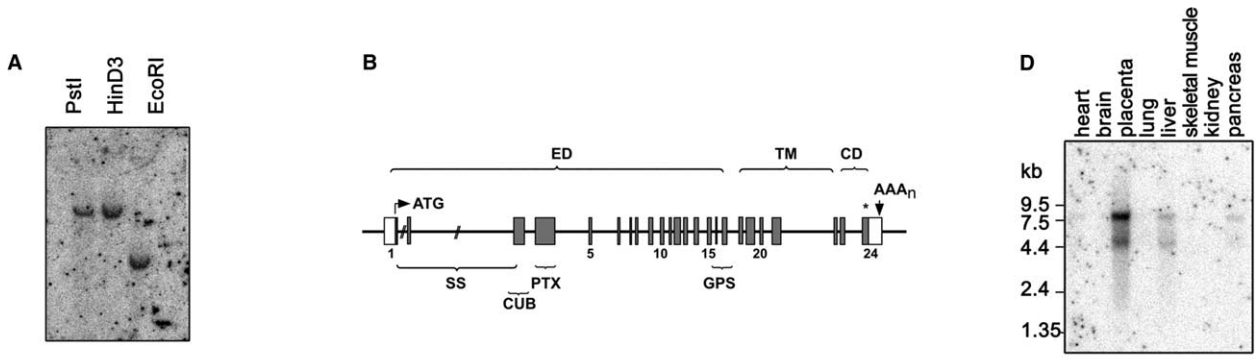

C

Intron/Exon	Size (bp)	cDNA Position	Intron-Exon-Intron boundary
Exon-1	418	1-418	
Intron-1	7213		AACAT-**GT**AAG...TGC**AG**-GATGT
Exon-2	100	419-519	
Intron-2	57924		CTCAG-**GT**AAG...AGC**AG**-TGTGG
Exon-3	341	520-861	
Intron-3	2259		CAGAG-**GT**ATG...CCT**AG**-TTGCC
Exon-4	623	862-1485	
Intron-4	11157		CTGTG-**GT**GAG...TCA**AG**-GTTCC
Exon-5	68	1486-1554	
Intron-5	8238		TCAAG-**GT**AGG...GGC**AG**-ATGGA
Exon-6	85	1555-1640	
Intron-6	2604		AATGG-**GT**AAG...TCC**AG**-CTCAA
Exon-7	52	1641-1693	
Intron-7	895		ATCAG-**GT**AAG...TTTT**AG**-TTTTC
Exon-8	62	1694-1756	
Intron-8	3654		CCAAG-**GT**AAC...CCT**AG**-GTTGG
Exon-9	142	1757-1899	
Intron-9	2729		ACTGG-**GT**AAG...TAT**AG**-GTCAT
Exon-10	111	1900-2011	
Intron-10	1397		ATATG-**GT**AAT...CAT**AG**-TTTTT
Exon-11	66	2012-2078	
Intron-11	560		CAAGG-**GT**GAG...AGA**AG**-AAGCA
Exon-12	208	2079-2287	
Intron-12	971		TCTGA-**GT**AAG...TTT**AG**-AGCTT

Intron/Exon	Size (bp)	cDNA Position	Intron-Exon-Intron boundary
Exon-13	171	2288-2459	
Intron-13	1715		TCCAG-**GT**AAT...GAC**AG**-ATGGA
Exon -14	140	2460-2600	
Intron-14	2321		TCCAG-**GT**AAG...AAA**AG**-GATGT
Exon-15	119	2601-2720	
Intron-15	1604		CTCAG-**GT**AAG...TAT**AG**-GAAGT
Exon-16	45	2721-2766	
Intron-16	3035		AAACG-**GT**AAG....AAC**AG**-AAGGT
Exon-17	152	2767-2873	
Intron-17	3557		TGATG-**GT**AAG...TGT**AG**-GACCT
Exon-18	127	2874-3001	
Intron-18	699		TTTGA-**GT**AAG...TTT**AG**-GAAAT
Exon-19	268	3002-3270	
Intron-19	1208		CTGGG-**GT**AAG...AAC**AG**-GTTTG
Exon-20	96	3271-3367	
Intron-20	2451		GAATT-**GT**AAG...TTA**AG**-CTGTT
Exon-21	283	3368-3651	
Intron-21	17329		ACAAG-**GT**AAG...CAC**AG**-GCTTA
Exon-22	101	3652-3753	
Intron-22	676		ACTCA-**GT**AAA...TTC**AG**-ATTGG
Exon-23	152	3754-3906	
Intron-23	4972		CACAG-**GT**GAG...TGC**AG**-ACAGT
Exon-24	616	3907-4523	

Fig. 3. Genomic organization of *VIGR*. (A) Southern blot of human genomic DNA, digested with either *Pst*I, *Hin*DIII, or *Eco*RI and hybridized with a cDNA specific to *VIGR*. (B) Human *VIGR* genomic organization. ED (extracellular domain), TM (transmembrane domain), CD (cytoplasmic domain), ss (signal sequence). An asterisk indicates the stop codon in human exon 24. (C) Intron/exon organization of human VIGR. Size of introns and exons as well as the cDNA position of exons are indicated. In addition, the sequence surrounding the intron–exon boundaries are shown, highlighting the conserved GT at the 5′end and the conserved AG at the 3′ end of the introns. Data were generated by aligning the VIGR cDNA sequence to the human genome sequence covering the long arm of chromosome 6. (D) Tissue distribution of *VIGR* mRNA. A multiple human tissue Northern-blot (Oncor) was hybridized with a ^{32}P labeled cDNA probe encoding *VIGR*. A RNA size marker is indicated on the left.

heptahelical region (7TM) or cytoplasmic domains (C1, C2). Immunoprecipitation of metabolically labeled and LPS treated HUVECs revealed a ~230 kDa protein which was specifically recognized. None of the antibodies recognized specific proteins in non-stimulated HUVECs. The difference in size to the predicted molecular weight of 136 kDa is probably due to extensive glycosylation of the extracellular domain, which was confirmed by treatment of HUVECs with tunicamycin, a potent inhibitor of N-glycosylation, resulting in a reduced molecular weight of ~136 kDa (Fig. 5A).

To demonstrate that VIGR is indeed expressed on the cell surface, we biotinylated surface proteins on HUVECs. Total protein lysates were immunoprecipitated and immune complexes were analyzed by SDS–PAGE/immunoblotting using streptavidin–peroxidase conjugates specific for biotinylated proteins. The 230 kDa VIGR protein was detected on the cell surface of LPS stimulated HUVECs, and pretreatment with tunicamycin reduced the molecular weight to ~136 kDa. No protein was detected on the surface of resting HUVECs (Fig. 5B). Moreover, the presence of under- or non-glycosylated forms at the cell surface shows that glycosylation is not essential for the cellular localization and seems not to impair intracellular transport of VIGR. VIGR expression on the cell surface of HUVECs is dose-dependent. Highest expression is detected using 600 ng/ml LPS in the medium, but 100 ng LPS are sufficient to induce VIGR expression. In contrast to VIGR, the LPS dependent expression of the EC activation marker ELAM-1 was constant under these experimental settings (Fig. 5C).

Additionally, we visualized VIGR expression on the cell surface by immunostaining of LPS stimulated HUVECs with VIGR antibodies, which recognize the extracellular domain of VIGR and a FITC-labeled secondary antibody. Immunofluorescence analysis showed cell membrane expression of VIGR (Fig. 6A and B), however, no staining was detected in quiescent HUVECs (Fig. 6C and D).

3.5. *Activation of mitogen-activated protein kinases (MAPKs), but not NF-κB results in inducible expression of VIGR in HUVECs*

In order to delineate the signaling pathways that are responsible for the inducible expression of VIGR in HUVECs,

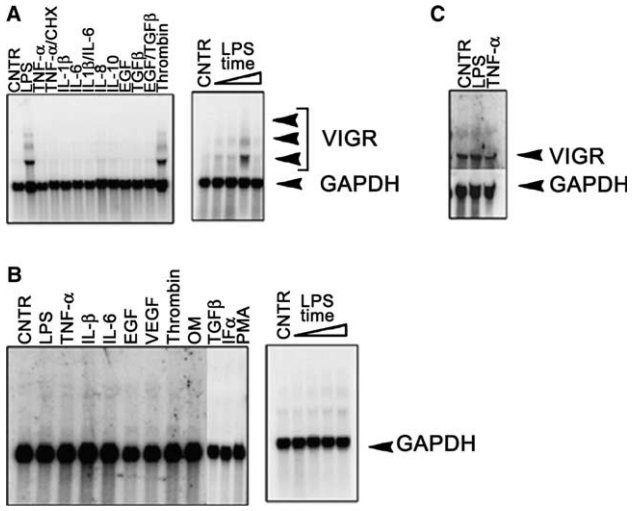

Fig. 4. *VIGR* expression in ECs. (A) Northern-blot analysis using total RNA isolated from HUVECs, treated for 9 h with the indicated stimuli (left panel) and a time course of *VIGR* expression in response to LPS (0, 4, 9, 12, and 24 h) (right panel). (B) An identical experiment was performed in human skin microvascular ECs (HSMECs). (C) *VIGR* mRNA expression in HAECs treated with LPS or TNFα for 8 h. A cDNA specific to human *GAPDH* was used simultaneously as a control. *VIGR* and *GAPDH* transcripts are indicated by arrows.

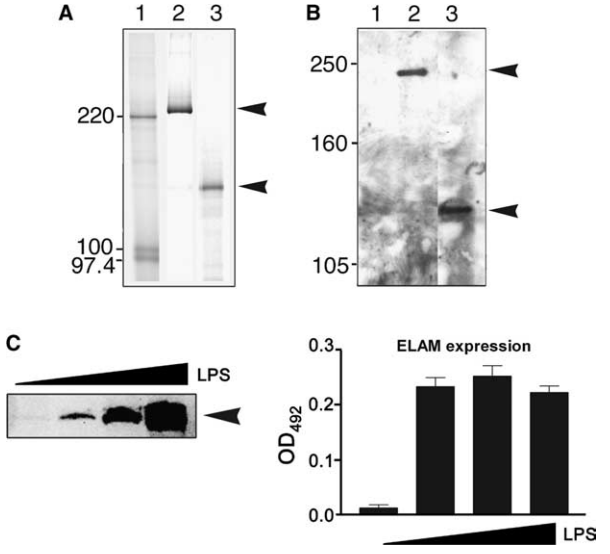

Fig. 5. Immunoprecipitation of VIGR. (A) HUVECs were metabolically labeled for 16 h in the presence of LPS (lane 2) or LPS and 4 μg/ml tunicamycin (lane 3). Total lysates were subjected to immunoprecipitation with anti-VIGR antibodies (C2) and bound immune complexes were separated by SDS–PAGE and detected by fluorography. A ^{14}C-labeled molecular weight standard is shown in lane 1. (B) Resting (lane 1) or 16 h LPS treated HUVECs in absence (lane 2), or presence of 4 μg/ml tunicamycin (lane 3), were surface biotinylated and subjected to immunoprecipitation using C2 antiserum. Immune complexes were separated by SDS–PAGE and analyzed by immunoblotting with streptavidin–peroxidase complexes. (C) Dose-dependent expression of VIGR on the cell surface of HUVECs in response to LPS. HUVECs were either left untreated, or were treated with 100, 300 and 600 ng/ml LPS for 16 h, and analyzed as above by surface biotinylation and immunoprecipitation [left panel]. For comparison, ELAM expression was determined by ELISA after stimulation with 0, 100, 300, and 600 ng/ml LPS for 4 h [right panel]. VIGR proteins are marked by arrows. All cell lysates were normalized for protein content.

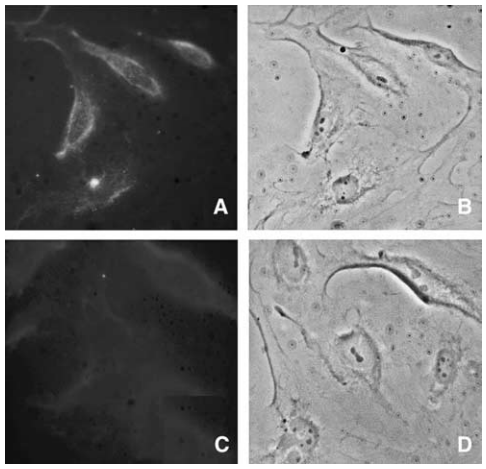

Fig. 6. Localization of VIGR in HUVECs. (A,B) HUVECs were either treated with LPS for 16 h or (C,D) left untreated. HUVECs were analyzed for VIGR expression using P4 antiserum and a FITC-labeled anti-rabbit secondary antibody. Cells were visualized directly by fluorescence microscopy (A,C), or by phase contrast (B,D).

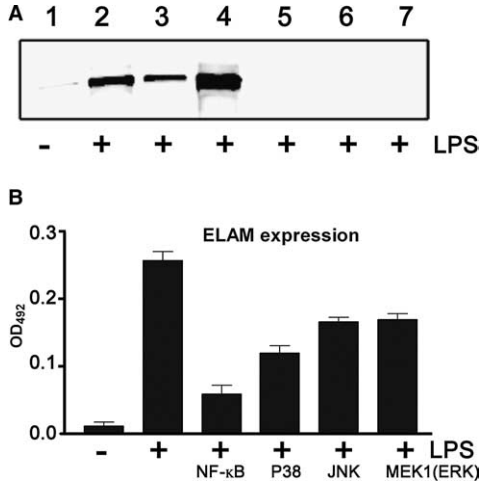

Fig. 7. Expression of VIGR on the cell surface in response to LPS is dependent on the combined activation of MAPK pathways. (A) HUVECs were either left untreated (lane 1) or were treated with LPS (200 ng/ml) for 16 h (lanes 2–7). Where indicated, specific chemical kinase inhibitors were applied 1 h prior to LPS treatment. Proteins were then surface biotinylated and VIGR was immunoprecipitated as described. NF-κB activation was inhibited with 5 μM of BAY11-7082 (lane 3); p38 activation was blocked with 40 μM of SB202190 (lane 4); activation of JNK was inhibited with 25 μM of SP600125 (lane 5); and MEK1 activation was blocked with 50 μM PD98059 (lane 6). As a specificity control, C2 pre-immune serum was employed in lane 7 in the immunoprecipitation step. (B) HUVECs were treated as above, but LPS treatment was reduced to 4 h to measure ELAM-1 expression by ELISA under these conditions. All cell lysates were normalized for protein content.

we employed chemical inhibitors specific for MAPK and NF-κB. We treated cells simultaneously with LPS and either the specific NF-κB inhibitor BAY11-7082, the specific MEK1 inhibitor PD98059, the specific p38 MAPK inhibitor SB202190, or the specific JNK inhibitor SP600125 for 16 h. Cell surface proteins were then specifically biotinylated and immunoprecipitation was performed as described above. Surprisingly, inhibition of the major pro-inflammatory transcription factor

NF-κB did not affect the inducibility of VIGR in response to LPS (Fig. 7, lane 3). However, specific inhibition of JNK and MEK1 (Fig. 7, lanes 5 and 6), but not p38 (Fig. 7, lane 4) MAPK pathways completely abolished VIGR expression in response to LPS in HUVECs (Fig. 7A). As a control, we determined expression of EC-specific adhesion molecule of the selectin family ELAM-1, a known NF-κB target gene, by ELISA under identical conditions. This adhesion molecule is tightly regulated in ECs and cytokine inducibility requires the co-operative interaction of NF-κB, ATF-2 and high mobility group I protein (Y) transcription factor complexes [25]. It was recently suggested that the ELAM promoter also contains an inducible AP-1/CREB site [26]. As shown in Fig. 7B, ELAM-1 expression is most sensitive to the NF-κB inhibitor BAY11-7082, whereas MAPK inhibitors are less potent in inhibiting ELAM-1 expression in HUVECs upon LPS treatment.

4. Discussion

We established a novel method for fast, simple and selective cloning of differentially expressed genes encoding secretory or membrane proteins. Using this approach we identified a novel cell surface receptor on ECs, which belongs to the adhesion family of GPCRs.

Most of the human adhesion GPCR family members are closely related on genetic level and found within the paralogon-3, which contains chromosomes 1/5p–q21/6p21–p25/9/15q11–q26/19p [4]. Moreover, the heptahelical region is formed by five exons instead of eight exons as usually found in the related secretin family of GPCRs. The heptahelical domain of VIGR is organized by five exons and localizes to paralogon-3.

Expression of VIGR varies with the type and origin of ECs. ECs derived from the microvasculature did not express VIGR. However, human aortic ECs (HAECs) showed constitutive basal expression and HUVECs displayed inducible expression in response to LPS and thrombin. This is of special note considering that LPS and thrombin may induce a large number of genes and complex cellular responses in ECs derived from large and small vessels [27]. Thrombin, a central protease of the coagulation pathway, initiates the final step in conversion of fibrinogen to fibrin and activates platelets to form a clot [28]. Increasing evidence suggests that the innate immune response and the coagulation system have coevolved and continue to function as highly integrated systems in response to injury and infection. Systemic inflammation is a potent pro-thrombotic stimulus by down-regulating anti-coagulant factors and inhibiting fibrin formation, while up-regulating pro-coagulant mediators and increasing platelet activity [29]. Moreover, acute inflammation occasionally results in systemic activation of the coagulation system, referred to as disseminated intravascular coagulation [27]. In addition of preventing thrombosis, anti-coagulatory factors also display an anti-inflammatory activity [30]. Apart from this, thrombin regulates expression of genes mediating mitogenesis, adhesion to leukocytes, and hemostasis [31]. Although genes induced by LPS or thrombin are rather diverse and cell type dependent, there is a subset of genes that can be induced by both stimuli. However, different signaling pathways are involved [31,32]. LPS mediated activation of NF-κB occurs through the toll-like receptor 4 complex, whereas thrombin acts through the activation of protease activated receptors. Most of the genes affected are mediators of the inflammatory response, controlled by NF-κB, which plays a pivotal role in activated ECs. Therefore, we conducted initial experiments using a recombinant adenovirus encoding inhibitor of NF-κB (IκBα) [33,34]. Ectopic expression of IκBα (data not shown), as well as inhibition of NF-κB activation employing chemical inhibitors, did not impair LPS induced expression of VIGR suggesting that activation of NF-κB is not involved. We suspected that VIGR expression might be controlled by other transcription factors, which would be consistent with the lack of VIGR induction by TNFα and IL-1β. Both, LPS and thrombin have been described to trigger NF-κB independent signaling pathways. Thrombin can activate gene expression via the JAK/STAT pathway, via a tyrosine kinase/DNA-binding protein pathway and via MAP kinase (MAPK) cascade leading to ERK2/Elk-1 activation [31]. Three MAPK pathways, JNK, ERK and p38 have been reported to be activated by LPS in macrophages and the latter two also in HUVECs [35]. Therefore we investigated, whether activation of MAPKs are required for inducible expression of VIGR in response to LPS in HUVECs. JNK and MEK1, the latter activates ERK1/2, MAPK signaling pathways are apparently both required for LPS-dependent inducible expression of VIGR in HUVECs, whereas activation of p38 does not result in VIGR expression. Consistently, analysis of the upstream promoter region also revealed potential AP-1, Egr-1 and Elk-1 consensus binding sites, but no NF-κB binding sites. Hence, we consider MAPKs to be a likely candidate involved in the transcriptional regulation of VIGR. All three MAPKs function in ECs and MAPK cross-talk likely plays an important role in EC activation [36]. The observation that VIGR is highly expressed in response to both induction of the innate immune response by LPS, as well as activation of the coagulation system by thrombin, suggests that VIGR functions at a converging step common to both pathways.

VIGR is unique because of its novel combination of extracellular adhesion motifs, namely CUB and PTX domains. The CUB domain is a ~110 amino acid residues extracellular domain that has been described for the first time in complement subcomponents (C1r/C1s), embryonic sea urchin protein 1 (Uegf) and bone morphogenetic protein 1 (Bmp1). CUB domain containing proteins are components and activators of the complement system, proteases responsible for cleavage of collagen [37], proteins mediating developmental processes [38], and even involved in cell-mediated immunity (attractin/DPPT-L) [39]. CUB domain proteins are either secreted or single transmembrane domain proteins, thus we report here the first GPCR containing a CUB domain. A recent report demonstrates, that CUB domain containing proteins are the most differentially regulated proteins in *Caenorhabditis elegans* larval development [40].

PTXs encompass the acute-phase plasma proteins human C-reactive protein (CRP) and serum amyloid P component. More recently some neuronal proteins and PTX3 (TSP14) have been reported to contain PTX domains. Classical PTXs form pentamers and decamers that show calcium-dependent binding to a variety of ligands such as bacteria, chromatin and carbohydrates. Many biological functions have been attributed to PTXs, including reactivity with the complement system and with phagocytic leucocytes, suggesting a role in natural host defense [41]. Noteworthy, PTX3 was demonstrated to be a pattern recognition receptor for the innate immune system fighting fungal infections [42].

Common to CUB and PTX domains is their calcium-dependent binding activity and both domains are linked to immune responses. The CUB domain has been reported to mediate association between C1s and C1r [43]. SAP forms a non-covalent complex with the C4b-binding protein, which regulates the classical complement pathway C3 convertase [44]. CRP was found to bind at the site of complement-induced injury and is believed to assist in clearance of extracellular debris during infection and inflammation [45]. Therefore it is tempting to speculate that VIGR might play an important role in innate immunity and inflammation by mediating cell–cell or cell–extracellular matrix interactions.

Recent evidence also links several adhesion GPCRs to cancer [6], and therefore, expression levels of VIGR in tumor cells should be addressed in the future.

Acknowledgements: We gratefully acknowledge David Blanco for providing plasmid pMG, Margarethe Geiger and Zydi Zhegu for immunization of rabbits and isolation of HSMECs and HUVEC, and Renate Hofer-Warbinek for providing the HM2, HM39/2, HM60, and HU2 cell lines. This work was supported by Biomolecular Therapeutics GmbH and a grant to J.L. from the Jubilaeumsfonds of the Austrian National Bank, Project 8114.

References

[1] Pober, J.S. (1988) Am. J. Pathol. 133, 426–433.
[2] Pierce, K.L., Premont, R.T. and Lefkowitz, R.J. (2002) Nat. Rev. Mol. Cell. Biol. 3, 639–650.
[3] Bockaert, J., Marin, P., Dumuis, A. and Fagni, L. (2003) FEBS Lett. 546, 65–72.
[4] Fredriksson, R., Lagerstrom, M.C., Lundin, L.G. and Schioth, H.B. (2003) Mol. Pharmacol. 63, 1256–1272.
[5] Hayflick, J.S. (2000) J. Recept. Signal Transduct. Res. 20, 119–131.
[6] Kwakkenbos, M.J., Kop, E.N., Stacey, M., Matmati, M., Gordon, S., Lin, H.H. and Hamann, J. (2003) Immunogenetics 55, 655–666.
[7] Stacey, M., Lin, H.H., Gordon, S. and McKnight, A.J. (2000) Trends Biochem. Sci. 25, 284–289.
[8] Fredriksson, R., Gloriam, D.E., Hoglund, P.J., Lagerstrom, M.C. and Schioth, H.B. (2003) Biochem. Biophys. Res. Commun. 301, 725–734.
[9] Krasnoperov, V., Lu, Y., Buryanovsky, L., Neubert, T.A., Ichtchenko, K. and Petrenko, A.G. (2002) J. Biol. Chem. 277, 46518–46526.
[10] Chang, G.W., Stacey, M., Kwakkenbos, M.J., Hamann, J., Gordon, S. and Lin, H.H. (2003) FEBS Lett. 547, 145–150.
[11] Stacey, M., Chang, G.W., Sanos, S.L., Chittenden, L.R., Stubbs, L., Gordon, S. and Lin, H.H. (2002) J. Biol. Chem. 277, 29283–29293.
[12] Abe, J., Fukuzawa, T. and Hirose, S. (2002) J. Biol. Chem. 277, 23391–23398.
[13] Gray, J.X. et al. (1996) J. Immunol. 157, 5438–5447.
[14] Obermann, H., Samalecos, A., Osterhoff, C., Schröder, B., Heller, R. and Kirchhoff, C. (2003) Mol. Reprod. Dev. 64, 13–26.
[15] Stacey, M., Lin, H.H., Hilyard, K.L., Gordon, S. and McKnight, A.J. (2001) J. Biol. Chem. 276, 18863–18870.
[16] Hamann, J., Stortelers, C., Kiss-Toth, E., Vogel, B., Eichler, W. and van Lier, R.A. (1998) Eur. J. Immunol. 28, 1701–1707.
[17] Stacey, M., Chang, G.W., Davies, J.Q., Kwakkenbos, M.J., Sanderson, R.D., Hamann, J., Gordon, S. and Lin, H.H. (2003) Blood 102, 2916–2924.
[18] Hamann, J., Vogel, B., van Schijndel, G.M. and van Lier, R.A. (1996) J. Exp. Med. 184, 1185–1189.
[19] Qian, Y.M., Haino, M., Kelly, K. and Song, W.C. (1999) Immunology 98, 303–311.
[20] Lin, H.H. et al. (2001) J. Biol. Chem. 276, 24160–24169.
[21] Blanco, D.R.G., M., Champion, C.I., Haake, D.A., Chikami, G.K., Miller, J.N. and Lovett, M.A. (1991) Mol. Microbiol. 5, 2405–2415.
[22] Osterhoff, C., Ivell, R. and Kirchhoff, C. (1997) DNA Cell Biol. 16, 379–389.
[23] Hamann, J. et al. (1995) J. Immunol. 155, 1942–1950.
[24] Vilardaga, J.P., Di Paolo, E., Bialek, C., De Neef, P., Waelbroeck, M., Bollen, A. and Robberecht, P. (1997) Eur. J. Biochem. 246, 173–180.
[25] Collins, T., Read, M.A., Neish, A.S., Whitley, M.Z., Thanos, D. and Maniatis, T. (1995) FASEB J. 9, 899–909.
[26] Jensen, L.E. and Whitehead, A.S. (2003) Biotechniques 35, 54–56.
[27] Levi, M., ten Cate, H. and van der Poll, T. (2002) Crit. Care Med. 30, S220–S224.
[28] Mann, K.G., Brummel, K. and Butenas, S. (2003) J. Thromb. Haemost. 1, 1504–1514.
[29] Opal, S.M. and Esmon, C.T. (2003) Crit. Care 7, 23–38.
[30] Esmon, C.T. (2003) J. Thromb. Haemost. 1, 1343–1348.
[31] Stenina, O.I. (2003) Curr. Drug Targets 4, 143–158.
[32] Bierhaus, A., Chen, J., Liliensiek, B. and Nawroth, P.P. (2000) Semin. Thromb. Hemost. 26, 571–587.
[33] Stehlik, C., de Martin, R., Kumabashiri, I., Schmid, J.A., Binder, B.R. and Lipp, J. (1998) J. Exp. Med. 188, 211–216.
[34] Wrighton, C.J., Hofer-Warbinek, R., Moll, T., Eytner, R., Bach, F.H. and de Martin, R. (1996) J. Exp. Med. 183, 1013–1022.
[35] Schumann, R.R., Pfeil, D., Lamping, N., Kirschning, C., Scherzinger, G., Schlag, P., Karawajew, L. and Herrmann, F. (1996) Blood 87, 2805–2814.
[36] Hoefen, R.J. and Berk, B.C. (2002) Vasc. Pharmacol. 38, 271–273.
[37] Hulmes, D.J., Mould, A.P. and Kessler, E. (1997) Matrix Biol. 16, 41–45.
[38] Bork, P. and Beckmann, G. (1993) J. Mol. Biol. 231, 539–545.
[39] Duke-Cohan, J.S., Tang, W. and Schlossman, S.F. (2000) Adv. Exp. Med. Biol. 477, 173–185.
[40] Gerstein, M. and Jansen, R. (2000) Curr. Opin. Struct. Biol. 10, 574–584.
[41] Gewurz, H., Zhang, X.H. and Lint, T.F. (1995) Curr. Opin. Immunol. 7, 54–64.
[42] Garlanda, C. et al. (2002) Nature 420, 182–186.
[43] Thielens, N.M., Enrie, K., Lacroix, M., Jaquinod, M., Hernandez, J.F., Esser, A.F. and Arlaud, G.J. (1999) J. Biol. Chem. 274, 9149–9159.
[44] Garcia de Frutos, P. and Dahlback, B. (1994) J. Immunol. 152, 2430–2437.
[45] Steel, D.M. and Whitehead, A.S. (1994) Immunol. Today 15, 81–88.